

Numerical Analysis of Aerodynamic Characteristics of a Corrugated MAV wing.

Prithwish Mukherjee
M. Tech. student
Department of Aerospace
Engineering,
Indian Institute of Technology,
Kharagpur.

M. Jaffar Mujawar
M. Tech. student
Department of Aerospace
Engineering,
Indian Institute of Technology,
Kharagpur.

Sandeep Saha*
Assistant Professor
Department of Aerospace
Engineering,
Indian Institute of Technology,
Kharagpur.

Abstract

This work is motivated by the idea of implementing corrugations found over dragonfly wings onto a flat plate airfoil to use it as a Low Aspect Ratio (LAR) wing for applications in Micro Air Vehicle (MAV) so as to utilize some added advantages of corrugations at low Reynolds Number (Re) such as higher lift and delayed onset of stall. The numerical investigation was carried out at a free-stream velocity of 15m/s, maintaining a Re of 10^5 using a commercial computational fluid dynamic (CFD) software. The maximum dimensions of the model were restricted to 20cm with an Aspect Ratio (AR) of 2. Finally, two designs were obtained which had delayed stall and one model had improved lift.

Keywords: *Corrugations, Low Aspect Ratio, Micro Air Vehicle, Low Reynolds Number, Computational Fluid Dynamics, Delayed Stall, Improved Lift.*

Introduction

From times as early as mankind thought of flying, the designers have always tried to imitate nature so as to obtain the advantages of a naturally flying creature. This mimicking of nature only led to the invention of aircraft and other airborne vehicles, but never has anyone been able to fully obtain the features of natural creatures. One such topic that is being researched extensively nowadays is corrugations.

Corrugations by definition are a series of crests (maxima) and troughs (minima) [1,2]. If the wing of a dragonfly is taken and cut through its cross section then it yields these series of crests and troughs. These can be considered as an airfoil and can be extruded to form a wing. Though the major portion of a dragonfly's flight profile consists of flapping, various research has already proven the advantages of this kind of profile in gliding as well [1-5]. Many insects have these kinds of corrugations in their wing structure [2,12] but the primary reason to select dragonfly's corrugation is based on a theory known as dynamic smoothing [2]. This phenomenon leads the dragonfly's wing to have a higher value of lift coefficient (C_L) by not affecting the drag much. Thus, this leads to an increment in lift as well as L/D. Further, though effects of corrugations are not sensitive to change in Re but it is specifically used in low Re regimes only because at high Re these corrugations produce excess drag by spoiling the streamlined nature of the flow and thus reduces the L/D. An experimental study conducted by Jeffery Murphy and Hui Hu at Iowa State University with the aim to analyze the utility of such a design in MAV application clearly showed that corrugated airfoils have a better performance over streamlined and flat plate airfoil at low Re regimes

* **Postal address:** Department of Aerospace Engineering, Indian Institute of Technology, Kharagpur, West Bengal- 721302, India.

* **E-mail:** ssaha@aero.iitkgp.ac.in

[4]. Similarly, it has also been observed that increasing the height of the corrugations too much can lead to increased drag and poor L/D whereas reducing the corrugation height too much reduces both lift and drag. So, another important aspect is to determine the height and number of corrugations on an airfoil to attain the desired characteristics [2,3].

For the present analysis, the basic wing geometry which was chosen is a replica of the design by Cosyn and Vierendeels [6] as shown in Fig. 1.a. The airfoil was a flat plate with thickness to chord ratio of 1.96%, a 5 to 1 leading edge and a sharp trailing edge which was extruded to form a rectangular wing. This wing was then redesigned with corrugations and the advantages of this design over the base designs were studied. The primary reason for selecting the work by Cosyn and Vierendeels [6] was the fact that they compared their results with the experimental data of Torres and Mueller [7]. This made the data provided by Cosyn and Vierendeels [6] to be more cogent. The design with AR=2 was chosen basically considering the fact that laminar separation stall becomes a major challenge for designs with $AR \leq 2$ whereas for $AR > 2$ designs, lift and drag are less severely affected by the tip vortices [6]. Thus, a trade-off was done and the AR=2 design was finalized.

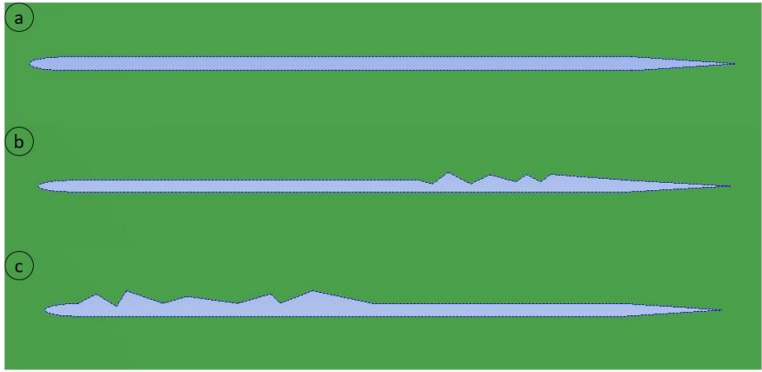


Figure 1. a. Cosyn and Vierendeels’[6] airfoil, b and c. airfoils of V1 and V2 respectively.

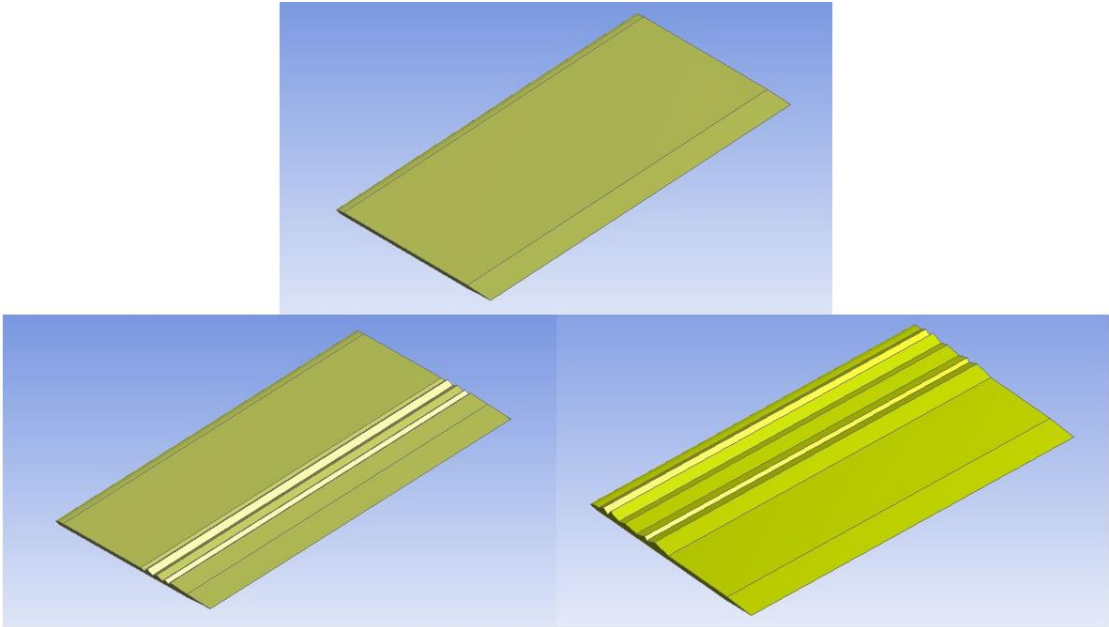


Figure 2. Cosyn and Vierendeels’[6] wing with AR=2 (top), V1 (bottom left) and V2 (bottom right).

The numerical analyses were performed at $Re=10^5$ primarily because the literature data were available at this Re only. Further reasons for selecting this particular Re are as follows. Firstly, for a wide range of mission, MAVs are required to fly up to a velocity of 20m/s [8,9]. But, an experimental investigation on corrugated airfoil conducted over a range of Re from 58,000-125,000, highlighted the fact that corrugated airfoils outperformed flat plate and streamlined airfoil at lower Re [4]. So, to keep the root chord Re at 58,000 approximately 8m/s velocity was required. Then, another experimental study by Dong-Ha Kim, et.al. highlighted the fact that linear variation of C_L was obtained above a Re of 1×10^5 , while below that Re lift coefficient was non-linear [10]. Considering all the above aspects, the free stream velocity was finalized to be 15m/s for these analyses which resulted in a maximum Re of approximately 1×10^5 .

As part of this work, two-dimensional tests were performed on the Cosyn and Vierendeels'[6] airfoil to check whether the solver settings were accurately predicting the results and thus validate our results in comparison to the literature data. Then two variations of corrugated airfoils were formed as an improvement to the initial airfoil as shown in Fig. 1 (b and c). Following this, further analyses were performed by forming three-dimensional rectangular wings out of the variations (b and c of Fig. 1) named as V1 and V2 (shown in Fig. 2) and compared with the AR=2 base wing of Cosyn and Vierendeels [6].

Finally, the improvements achieved in comparison with the initial flat rectangular wing were recorded. Several two-dimensional studies on corrugated airfoils have already yielded sufficient data to prove the advantages of these designs for low Re applications as compared to other conventional airfoils and so this particular work is only focussed towards the behavior of such corrugations in three dimensions.

Computational Analysis

The designs were made and computations were performed in commercial software namely Design Modeler and FLUENT of ANSYS 18.2 academic package respectively.

- A. Design:** As mentioned earlier, the geometry was designed to have an AR=2 and maximum dimensions of 20cm. Thus, the wing with flat plate airfoil was designed to have a rectangular planform with span of 20cm and chord of 10 cm. Similarly, the corrugated variations were also designed into wings with AR=2.

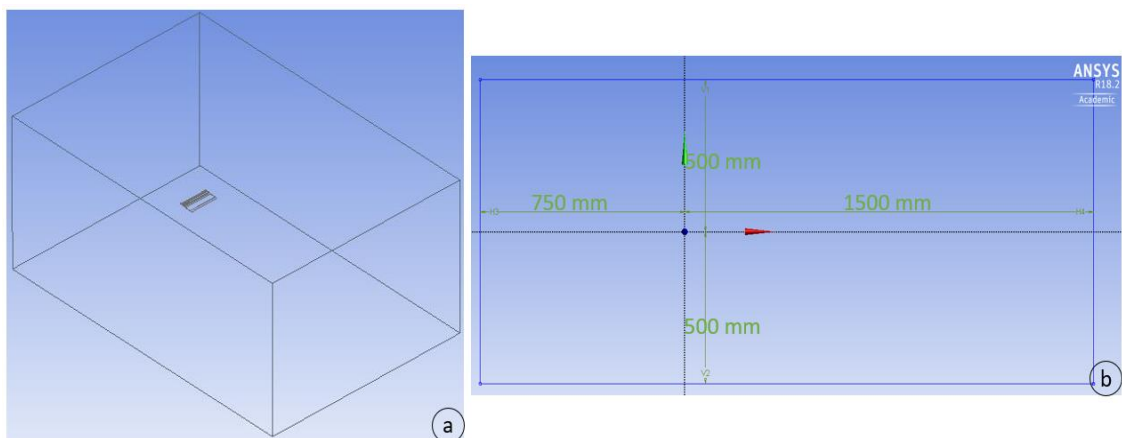


Figure 3. a. Domain (isometric view), b. Two-dimensional view of the domain.

An important consideration for designing the corrugated variations was that the bottom surface corrugations do not play an important role in increasing the lift [3]. Thus, for both the variations the bottom surface of the base airfoil was kept intact. For the First Variation (V1), the corrugations were applied from 55% of the root chord only on the top surface. The corrugations were not applied on the initial part of the airfoil with the conjecture so as not to destroy the suction peak negative pressure coefficient formed at around quarter chord location of the airfoil. Counterintuitively, the Second Variation (V2) was designed to have corrugations in the initial half of the wing only till 50% of the root chord and a smooth latter half. The crux of the analysis was to determine the advantages of these two models over one another and also compared to the initial rectangular wing.

B. Domain and Mesh details: A large rectangular domain was set so as to prevent any kind of interactions from the walls (shown in Fig. 3.a). Rectangular (cuboid) domain was preferred over other shapes because it was found to result in better convergence of the residuals. The inlet was set 750mm from the nose of the wing and the outlet of the domain was set 1500mm from the nose. Top and bottom walls were set at 500mm from root chord (shown in Fig. 3.b). This was then extruded from the root chord on both sides to 750mm giving a total thickness of 1500mm. For airfoil analysis, the two-dimensional mesh is of the same dimensions as mentioned above.

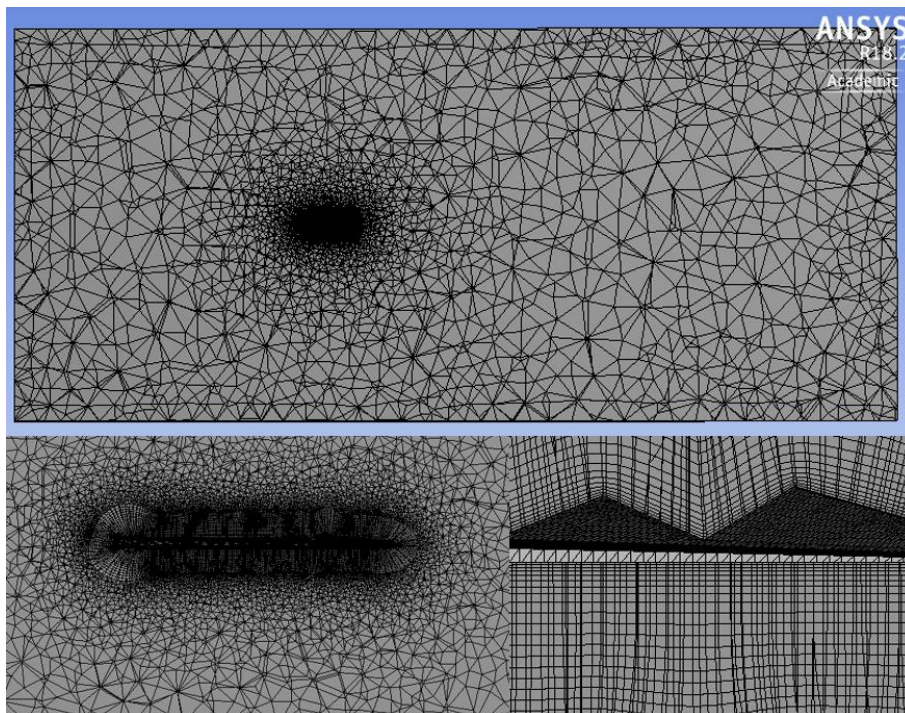


Figure 4. Cut section view of the meshed domain (top), followed by zoomed in view of the wing mesh (bottom left) and the view of the first layer thickness (bottom right).

For all the analyses an unstructured mesh is used with a sphere of influence around the wing (shown in Fig. 4). Element size in the sphere of influence was maintained to be 5×10^{-4} m and an approximate y^+ value of 5 was maintained just adjacent to the surface by using first layer thickness of 1×10^{-4} m having 25 layers with a growth rate of 1.2 (shown in Fig. 4).

C. **Analysis set-up:** FLUENT uses a finite-volume approach to solve incompressible Reynolds averaged Navier-Stokes equation. The present computations were made assuming steady state and neglecting gravity effects using second-order accurate, Semi-Implicit Method for Pressure-Linked Equations-Consistent (SIMPLEC) scheme. A $k-\omega$ based Shear Stress Transport (SST) model was used for turbulence modeling with the speculation that the flow becomes turbulent when interacting with the corrugations. The primary reason for using $k-\omega$ -SST model was due to its advantages of analyzing both near wall as well as free stream flows accurately [11].

Grid sensitivity tests were performed by using twice the element size (i.e., half the number of cells) as well as half the element size (or, twice the number of cells) as compared to the present grid. The accuracy of the C_L value of the rectangular wing at $\alpha = 5^\circ$ was used as the parameter to finalize the grid size. For half the number of cells, the C_L value was accurate in the order of 10^{-1} whereas for twice the number of cells the C_L value of the present grid were similar to the order of 10^{-3} . Thus, the present grid specification was selected as compared to the finer one so as to reduce the computational time.

D. **Boundary definition:** In accordance with our earlier discussions in the introduction section, the inlet of the domain was defined with a uniform velocity inlet of 15m/s. The outlet of the domain was defined to be a pressure outlet with zero gauge pressure and used the values upstream to derive its data. The walls of the domain and wing models were defined to be walls with no-slip boundary condition.

Another important consideration made for all the analyses was that all the data obtained were from numerical analysis till an angle of attack (α) of 15° . It is primarily because the main aim of this endeavour is to estimate the improvement of cruise performance of MAVs and MAVs generally cruise at angles much lesser than 10° [8,13]. Further, the data available for comparison from the literature were restricted to $\alpha = 15^\circ$, because sththe all was reached approximately around that angle [6]. Beyond stall, the steady state assumption fails to hold [6,14] and thus the simulations performed with the present solver settings will either not give a converged result or will result in an inaccurate prediction.

Validation of the solving technique

Validation of the numerical model was done by comparing the aerodynamic characteristics such as lift coefficient (C_L) and drag coefficient (C_D) to the results obtained by Cosyn and Vierendeels [6] as well as Torres and Mueller [7] (shown in Fig. 5).

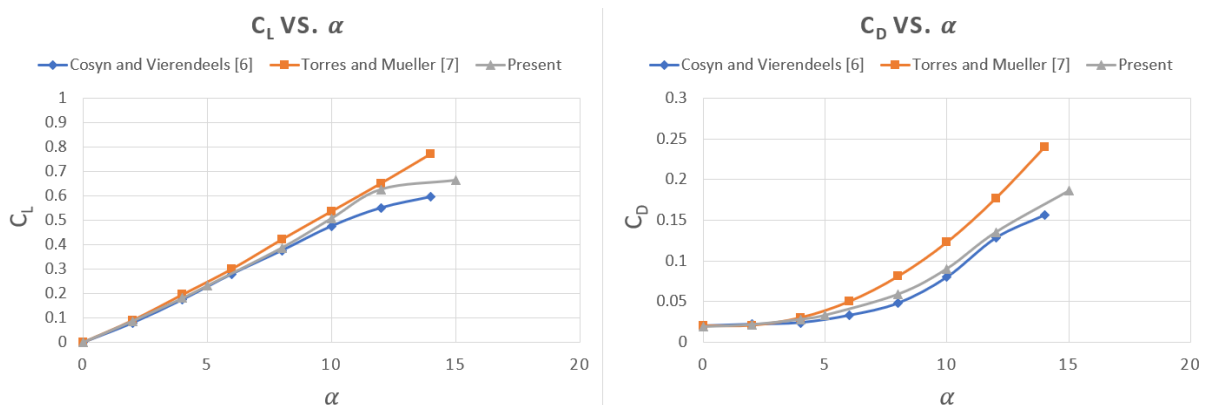


Figure 5. Comparison of aerodynamic characteristics of AR=2, flat, rectangular wing obtained through specified solver and literature.

As seen from the figure 5, both C_L and C_D calculated by the present solver settings are in reasonable agreement with that obtained by both Cosyn and Vierendeels [6] as well as Torres and Mueller [7], particularly at a lower angle of attack. Thus, the numerical method was validated for other analyses.

Results and Discussions

The aerodynamic characteristics were analyzed and parameters such as C_L and C_D were plotted with respect to the angle of attack (α) (shown in Fig. 6). It is clear from the C_L Vs. α plot that at cruise conditions, all the wings have almost the same performance. Moving towards higher angles of attack shows that V1 has almost same C_L as that of the rectangular wing whereas V2 certainly has an increment in C_L as compared to both the other designs and this difference increases as one moves to higher angles of attack. Further, the C_D plot (shown in Fig. 6) also provides some useful information. All the three wings have almost similar C_D Vs. α distribution but the V2 design has an increased value of drag at all angles. A better insight into the achieved C_L can be obtained by careful analysis of the coefficient of pressure (C_P) distribution along root airfoil of the respective wings at $\alpha=5^\circ$ (shown in Figs. 7,8 and 9).

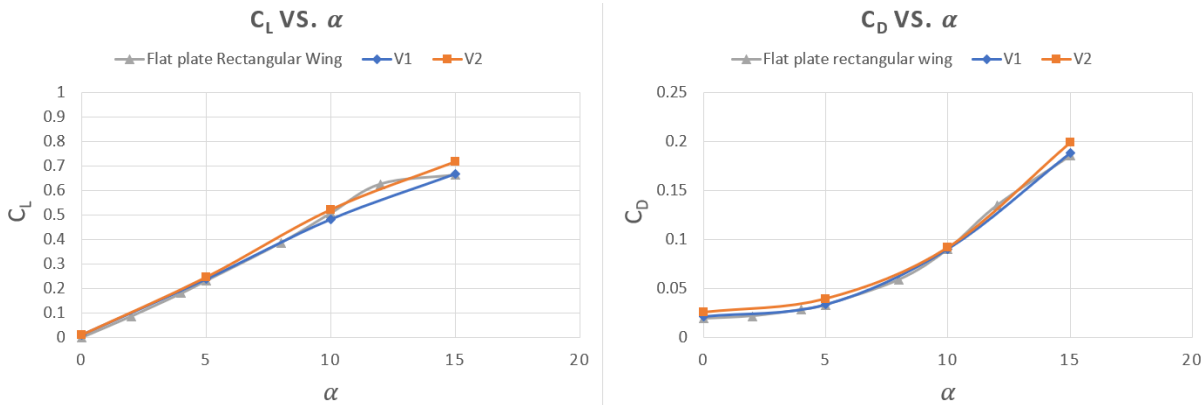


Figure 6. Plot showing Aerodynamic Characteristics of AR=2, flat plate rectangular wing and modified designs V1 and V2.

Primarily, focussing on the C_P distribution along the root chord of Cosyn and Vierendeels’[6] rectangular wing (shown in Fig. 7), we notice that the top surface has a peak negative pressure coefficient of 1.9 near the nose and this is attributed to the elliptical leading edge used by Torres and Mueller. Following that there is almost smooth distribution all over except a small negative kink at the rear end possibly due to the sharp trailing edge. The bottom surface similarly has a sharp positive pressure coefficient near the leading edge followed by an almost smooth positive profile backed by a small negative kink.

Then, we move on to analyze the C_P distribution along the root chord of V1 (shown in Fig. 8). It is quite interesting to note that before the corrugations start the C_P distribution is almost similar to the previous design but as soon as the flow encounters the corrugations, it is clearly noticeable that the corrugated part has a better negative C_P distribution over the top surface while not tampering with the bottom surface distribution. This leads to the marginal C_L increment as mentioned earlier.

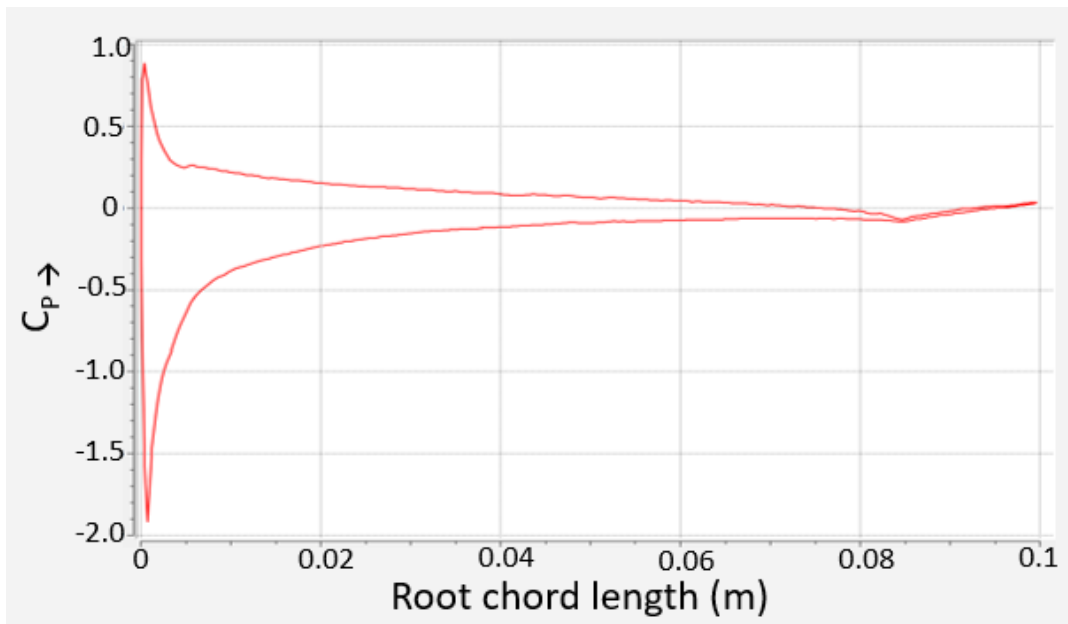


Figure 7. Plot showing C_p distribution over the root chord of Cosyn and Vierendeels' [6] rectangular wing.

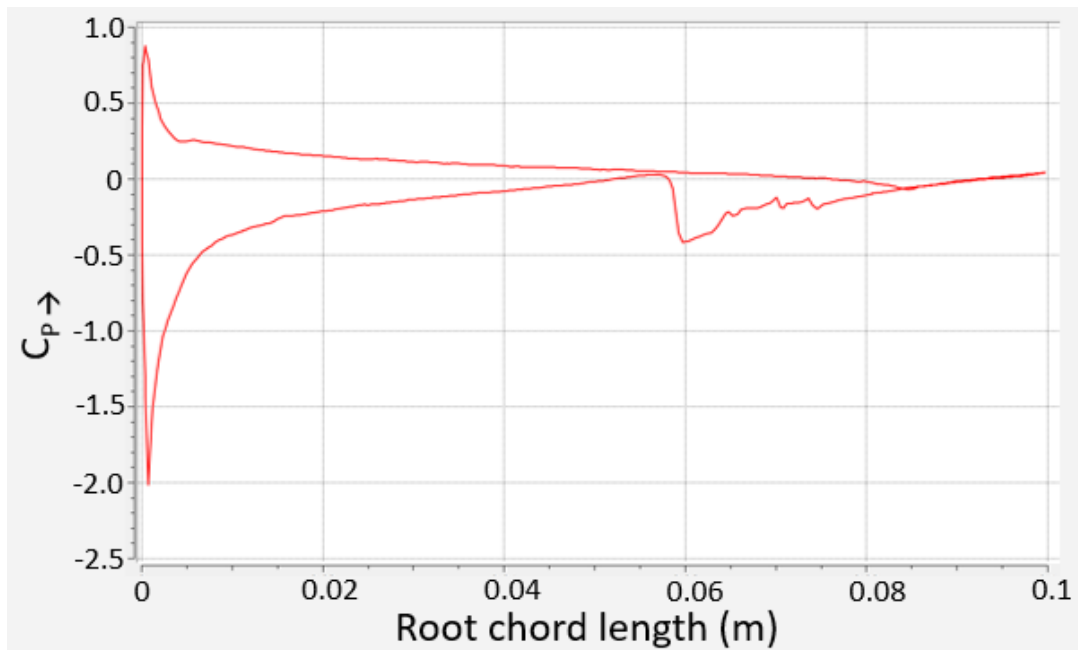


Figure 8. Plot showing C_p distribution over the root chord of V1 wing.

Finally, the analysis of C_p distribution plot across the root chord of V2 (shown in Fig. 9) gives us some important insights. Firstly, as this variation has corrugations form the leading edge, the magnitude of the peak negative coefficient has decreased to almost 1 which is half of the previous values. But, on careful observations one might

be clearly able to identify that though this variation has a lesser peak negative pressure coefficient, this airfoil actually has a much better distribution of suction pressure coefficient about its top surface while the bottom surface has similar positive pressure distribution like the others. This fact leads to the availability of the excess C_L found in Fig. 6.

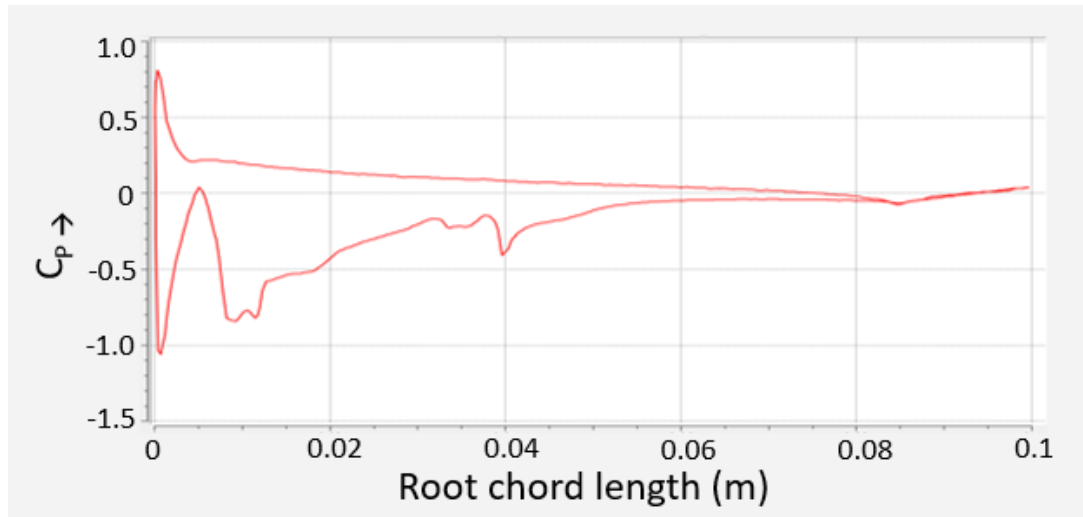


Figure 9. Plot showing C_p distribution over the root chord of V2 wing.

One very interesting fact that came out through this effort was that according to Cosyn and Vierendeels [6], their AR=2 wing was stalling at around 15° and the similar conclusion came out from the present analysis also (shown in Fig. 6). But if we see the trend of the C_L Vs. α for V1 and V2, we notice that the curves are almost straight instead of flattening out like simple rectangular wing even at angles as high as 15° . Thus, it might be possible that both these variations have delayed onset of stall however, a transient simulation might provide further insight into the stall characteristics.

Conclusion

A Low Reynolds number, LAR wing form literature was analyzed using a commercial CFD software. Then the validated numerical method was used to analyze the flow over two different variations of corrugated wings. Finally, both variations suggested probable improvement in stall characteristics with almost similar aerodynamic characteristics. Therefore, though not much improvement in aerodynamic efficiency (L/D) is expected in any of the variations, other characteristics like stalling angle and moments are worth investigating.

Further, for accurate prediction of stall angle and post stall characteristics, transient state simulations can be performed. This can help obtain a more accurate prediction of stall angle as well as $C_{L,max}$ for potential application in MAV designs.

References

- [1] Kesel, A. B., “Aerodynamic characteristics of dragonfly wing sections compared with technical aerofoils,” *The Journal of Experimental Biology*, Vol. 203, 2000, pp. 3125–3135.
- [2] Kim, W. K., Ko, J. H., Park, H. C., and Byun, D., “Effects of corrugation of the dragonfly wing on gliding performance,” *Journal of Theoretical Biology*, Vol. 260, No. 4, 2009, pp. 523–530. doi:10.1016/j.jtbi.2009.07.015.
- [3] Jain, S., Bhatt, V. D., and Mittal, S., “Shape optimization of corrugated airfoils,” *Journal of Computational Mechanics*, Vol. 56, No. 6, 2015, pp. 917–930. doi:10.1007/s00466-015-1210-x.
- [4] Jeffery Murphy and Hui Hu, “An Experimental Investigation on a Bio-inspired Corrugated Airfoil,” 47th AIAA Aerospace Sciences Meeting and Exhibit, Airfoil/Wing/Configuration Aerodynamics, American Institute of Aeronautics and Astronautics, Orlando, Florida, 7th January, 2009.
- [5] Wakeling, J. M., and Ellington, C. P., “Dragonfly flight. I. Gliding flight and steady-state aerodynamic forces,” *The Journal of Experimental Biology*, Vol. 200, 1997, pp. 543–556.
- [6] P. Cosyn and J. Vierendeels, “Numerical Investigation of Low-Aspect-Ratio Wings at Low Reynolds Numbers,” *JOURNAL OF AIRCRAFT*, Vol. 43, No. 3, 2006, pp. 713–722. doi:10.2514/1.16991.
- [7] Torres, G. E., and Mueller, T. J., “Low-Aspect-Ratio Wing Aerodynamics at Low Reynolds Numbers,” *AIAA JOURNAL*, Vol. 42, No. 5, 2004, pp. 865–873. doi:10.2514/1.439.
- [8] Dr. Dilek Funda Kurtulus, “Recent developments in unmanned aircraft systems (UAS, including UAV and MAV)”, Chapter 7, Published by Von Karman Institute of Fluid Dynamics, 2011, pp. 219-255.
- [9] Mohd. Shariff Ammoo and Md. Nizam Dahalan, “Micro Air Vehicle: Technology Review and Design Study,” 1st Regional Conference on Vehicle Engineering & Technology, Kuala Lumpur, Malaysia, 2006.
- [10] Kim, D.-H., Chang, J.-W., and Chung, J., “Low-Reynolds-Number Effect on Aerodynamic Characteristics of a NACA 0012 Airfoil,” *JOURNAL OF AIRCRAFT*, Vol. 48, No. 4, 2011, pp. 1212–1215. doi:10.2514/1.C031223.
- [11] David Monk and Dr. Edmund A. Chadwick, “Comparison of Turbulence Models Effectiveness for a Delta Wing at Low Reynolds Numbers,” 7th European Conference for Aeronautics and Space Sciences, Milan, Italy, July 2017.
- [12] Willmott, A. P., “The mechanism of hawkmoth flight,” Ph.D. thesis, Cambridge University, 1995.
- [13] Mostafa Hassanalian and Abdessattar Abdelkefi, “Design and manufacture of a fixed wing MAV with Zimmerman planform”, 54th AIAA Aerospace Sciences Meeting, San Diego, California, USA, January 2016.
- [14] John D. Anderson, Jr., “Fundamentals of Aerodynamics,” 6th Edition, Part 4, chapter 15, Published by McGraw-Hill Education, 2017, pp. 925-935.